

Linear optical properties of a heavily Mg-doped $\text{Al}_{0.09}\text{Ga}_{0.91}\text{N}$ epitaxial layer

M. J. Bergmann,^{a)} Ü. Özgür, and H. C. Casey, Jr.

Department of Electrical and Computer Engineering, Box 90291, Duke University, Durham, North Carolina 27708-0291

J. F. Muth, Y. C. Chang, and R. M. Kolbas

Department of Electrical and Computer Engineering, Box 7911, North Carolina State University, Raleigh, North Carolina 27695-7911

R. A. Rao and C. B. Eom

Department of Mechanical Engineering and Materials Science, Box 90300, Duke University, Durham, North Carolina 27708-0300

M. Schurman

Emcore Corporation, 394 Elizabeth Avenue, Somerset, New Jersey 08873

(Received 18 September 1998; accepted for publication 29 March 1999)

The room-temperature absorption coefficient and ordinary refractive index for a $\sim 0.4\text{-}\mu\text{m}$ -thick p -type wurtzite $\text{Al}_{0.09}\text{Ga}_{0.91}\text{N}$ epitaxial layer were determined via optical transmission measurements. The layer was grown by metal organic chemical vapor deposition and heavily doped ($\sim 5 \times 10^{19} \text{ cm}^{-3}$) with Mg. Additional measurements of the refractive index by prism coupling to the layer confirmed the transmission results. The low-temperature AlN buffer layer altered the expected interference fringes of the transmission spectrum below the band-gap energy and had to be accounted for in the analysis. The absorption coefficient exhibited band-tail effects and had a reduced slope near band-gap energy as compared to undoped GaN. Using a detailed balance argument, the reduced slope was consistent with the lack of a peak in the continuous-wave photoluminescent emission. © 1999 American Institute of Physics. [S0003-6951(99)00321-6]

In nitride-based laser diodes (LDs), $\text{Al}_x\text{Ga}_{1-x}\text{N}$ is used as cladding layers to provide confinement of the optical field. In order to achieve low resistivity p -type cladding layers, which minimize heating of the LDs, high doping levels are needed, with doping levels in the range 10^{19} – 10^{20} cm^{-3} producing resistivities on the order of $1.0 \text{ }\Omega \text{ cm}$ for GaN:Mg.¹ The effects of such high doping levels on the optical properties of the cladding layers are particularly important in LDs due to the penetration of the optical field into the cladding layers.^{2,3} Other authors have reported the ordinary refractive index $n(\lambda)$ and the absorption coefficient $\alpha(\lambda)$ of nominally undoped $\text{Al}_x\text{Ga}_{1-x}\text{N}$ ($0.0 \leq x \leq 1.0$),⁴ whereas the $\text{Al}_{0.09}\text{Ga}_{0.91}\text{N}$ layer reported on here is heavily Mg doped, which is typical of p -type cladding layers in current LDs. In this letter, $n(\lambda)$ and $\alpha(\lambda)$ are reported for an $\text{Al}_{0.09}\text{Ga}_{0.91}\text{N}$:Mg epitaxial film of thickness $\sim 0.4 \text{ }\mu\text{m}$. An expression for the transmittance that includes the buffer layer was derived and is used to determine $n(\lambda)$ and $\alpha(\lambda)$.

The film was grown by Emcore Corporation on a (0001) oriented two-inch double-polished sapphire substrate. An AlN buffer layer was deposited at low temperature ($\sim 600 \text{ }^\circ\text{C}$) prior to the low-pressure growth of the $\text{Al}_{0.09}\text{Ga}_{0.91}\text{N}$:Mg layer. The average Mg concentration was approximately $5 \times 10^{19} \text{ cm}^{-3}$ as determined by secondary ion mass spectroscopy (SIMS).⁵ The chemical composition of the solid solution was determined by Auger electron spectroscopy (AES).⁵ The transmission data were taken at normal incidence with a dual-beam Cary 5E spectrophotometer.⁶

The data presented here are for the sample unannealed. After annealing at $\sim 750 \text{ }^\circ\text{C}$ for four minutes in a N_2 atmosphere, the transmission spectrum and surface morphology did not change significantly.

The $\text{Al}_{0.09}\text{Ga}_{0.91}\text{N}$:Mg film and buffer layer produced a modulation of the optical transmission spectrum through interference of multiple reflections from the boundaries of the layers. The optical transmission data in Fig. 1 (solid line) is inconsistent with the model of a single thin film on a thick substrate that has been used to extract $n(\lambda)$ and $\alpha(\lambda)$ from transmission data.^{4,7,8} The reduction in magnitude of the in-

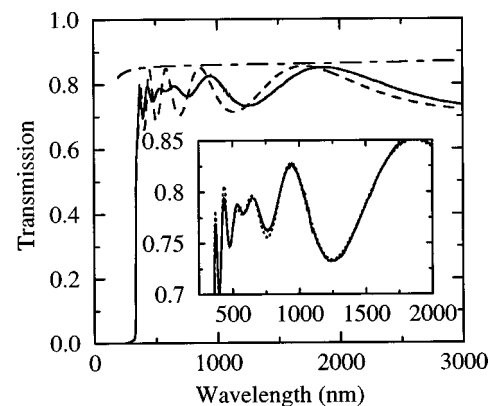


FIG. 1. Transmission spectrum at room temperature for an $\text{Al}_{0.09}\text{Ga}_{0.91}\text{N}$:Mg film on a sapphire substrate with an AlN buffer layer. The solid line is the transmission data, the dashed line is the calculated transmission spectrum using the parameters in Table I, except with $d_2 = 0 \text{ nm}$ (no buffer layer). The dot-dashed line is the interference-free transmission calculated for the sapphire substrate alone. In the inset, the dotted line is the fitted transmission with $d_2 = 69.7 \text{ nm}$.

^{a)}Electronic mail: mjb@ee.duke.edu

terference fringes that is most pronounced for $\lambda \approx 600$ nm cannot occur in a model of single uniform film, nor can the increase in magnitude of the local minima be accounted for. Measurements of other $\text{Al}_x\text{Ga}_{1-x}\text{N}$ films on both AlN and GaN buffer exhibited similar behavior, making it likely that this pinching of the interference fringes is a general phenomena. Two modifications to the single film model can account for these effects: a linear variation in the film thickness^{9,10} or the presence of a second layer with a different refractive index from the film layer. Atomic force microscopy (AFM) revealed a root-mean-square (rms) surface roughness of ~ 10 nm with isolated peaks of ~ 60 nm. This amount of surface roughness could not account for the modulation of the single film transmission spectrum. The more probable source of the modulation is a second thin layer, namely the AlN buffer layer.

The matrix formulation of boundary conditions for the electric fields at the layer interfaces was used to calculate the transmittance $T(\lambda)$ of the air-film-buffer-substrate-air stack.^{11,12} Absorption was included only in the film layer and interference effects were neglected in the thick substrate. The expression for $T(\lambda)$ for just the film-buffer layers is complicated in part due to the complex refractive index of the film, $\hat{n}(\lambda) = n(\lambda) - ik(\lambda)$, where $k(\lambda)$ is the extinction coefficient. For energies below the band-gap energy, $k \ll n$; therefore, the simplification $k=0$ can be made except where k appears as an exponent.⁷ The resulting transmittance $T_1(\lambda)$ through the air-film-buffer layers is

$$T_1 = 16n_1^2 s x [(c_1^2 + c_2^2 x^2 + 2c_1 c_2 x \cos 2\delta_1) \cos^2 \delta_2 + (c_3^2 + c_4^2 x^2 + 2c_3 c_4 x \cos 2\delta_1) \sin^2 \delta_2 + (c_1 c_4 - c_2 c_3) x \sin 2\delta_1 \sin 2\delta_2]^{-1}, \quad (1a)$$

where

$$c_1 = (n+s)(1+n), \quad c_2 = (n-s)(1-n), \quad (1b)$$

$$c_3 = \left(n_2 + \frac{ns}{n_2} \right) (1+n), \quad c_4 = \left(\frac{ns}{n_2} - n_2 \right) (1-n), \quad (1c)$$

$$\delta_1 = \frac{2\pi}{\lambda} n d, \quad \delta_2 = \frac{2\pi}{\lambda} n_2 d_2, \quad x = \exp -\alpha d. \quad (1d)$$

The thickness and refractive index of the film and buffer layer are d and n and d_2 and n_2 , respectively. The transmittance $T_2(\lambda)$ through the substrate-air interface is

$$T_2 = \frac{4s}{(1+s)^2}. \quad (2)$$

Accounting for multiple reflections in the substrate and absorption in the film lead to the final expression for the transmittance through all layers,

$$T = \frac{T_1 T_2}{(1-x) + T_1 + x T_2 - T_1 T_2}. \quad (3)$$

To perform a fit to Eq. (3) it is necessary to assume functional forms for $n(\lambda)$, $n_2(\lambda)$, and $\alpha(\lambda)$. An approach that does not require such assumptions, as in Ref. 7 for a single layer, is not possible due to the additional parameters

TABLE I. Results of fit to the transmission spectrum.

Parameter	Value
A_1	3.962 ± 0.003
λ_1	181 ± 3 nm
d	379 ± 1 nm
A_2	3.00 ± 0.03
λ_2	120 ± 20 nm
d_2	69.7 ± 0.1 nm
α_0	222.5 ± 0.5 cm ⁻¹
α_1	$2 \times 10^{-7} \pm 1 \times 10^{-7}$ cm ⁻¹
λ_α	8500 ± 300 nm

introduced by the buffer layer. First-order Sellmeier dispersion formulas were assumed for $n(\lambda)$ and $n_2(\lambda)$,¹³

$$n^2 = 1 + \frac{A_1 \lambda^2}{\lambda^2 - \lambda_1^2}, \quad n_2^2 = 1 + \frac{A_2 \lambda^2}{\lambda^2 - \lambda_2^2}, \quad (4)$$

where A_1, A_2, λ_1 , and λ_2 are adjustable parameters. The absorption coefficient is assumed to have a background constant value and an Urbach-tail region near the band-gap energy,¹⁴

$$\alpha(\lambda) = \alpha_0 + \alpha_1 \exp \frac{\lambda_\alpha}{\lambda}, \quad (5)$$

where α_0, α_1 , and λ_α are adjustable parameters. Equation (3) was fit to the transmission data via minimization of χ^2 using a Levenberg-Marquardt algorithm. The fitted parameter values are given in Table I and the corresponding transmittance is the dotted line in the inset of Fig. 1. The importance of including the buffer layer is illustrated by comparing the agreement between the dotted line and the transmission in the inset to that of the dashed line and the transmission in the main area of Fig. 1. The only difference between the two lines is that $d_2=0$ for the dashed line. Without the buffer layer, the observed ‘‘pinching’’ of the transmittance spectrum cannot be explained.

The dispersion of $n(\lambda)$ shown in Fig. 2(a) is in reasonable agreement with the measurement of undoped $\text{Al}_{0.11}\text{Ga}_{0.89}\text{N}$ by Brunner *et al.*⁴ given the assumptions of our model, the unknown effects of heavy doping, and possible uncertainty in the determinations of the Al mole fractions. A second independent measurement of $n(\lambda)$ was performed by coupling light from Ar⁺, HeNe, and semiconductor lasers into the film layer (waveguide layer) via a TiO₂ prism.^{15,16} The coupling data are indicated by filled circles in Fig. 2(a) and show good agreement with $n(\lambda)$ as determined by the transmission fit. Figure 2(b) compares $n_2(\lambda)$ to the dispersion for crystalline AlN,⁴ the low value of $n_2(\lambda)$ may be due to the noncrystalline nature of the layer, defects, and/or low density. The total thickness of the film and buffer layers was determined to be ~ 455 nm via mechanical profiling, which agrees well with the fit results.

In the region of strong absorption ($\lambda \lesssim 350$ nm), the interference effect was unobservable and the effect of the buffer layer was ignored. The absorption spectrum was then analyzed with the simpler method of multiple planar layers.¹⁷ The combined results of the analyses for $\alpha(\lambda)$ in the regions of weak and strong absorptions are plotted as the solid line in Fig. 2(c), with the absorption coefficient for undoped GaN

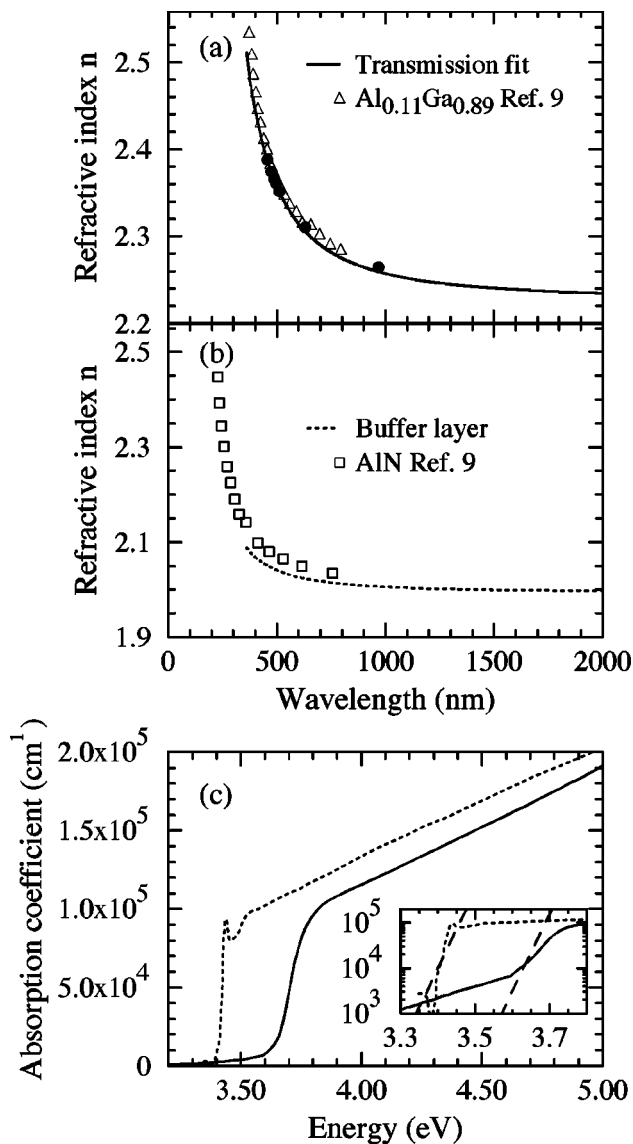


FIG. 2. (a) The solid line is the ordinary refractive index of $\text{Al}_{0.09}\text{Ga}_{0.91}\text{N}:\text{Mg}$ as determined by fitting to the transmission spectrum and the filled circles are determined by prism coupling. The triangles are for undoped $\text{Al}_{0.11}\text{Ga}_{0.89}\text{N}$ from Ref. 4. (b) The dotted line is the fit for the buffer layer and the squares are for undoped AlN from Ref. 4. (c) The absorption coefficients for $\text{Al}_{0.09}\text{Ga}_{0.91}\text{N}:\text{Mg}$ (solid line) and undoped GaN from Ref. 6 (dotted line). The inset includes two dashed lines that are proportional to $\exp(h\nu/(kT))$.

plotted for comparison.⁶ The strong excitonic effect in the GaN film, which resulted in the peak near the band-gap energy, was not present in the $\text{Al}_{0.09}\text{Ga}_{0.91}\text{N}:\text{Mg}$ film and the slope of the absorption edge in the $\text{Al}_{0.09}\text{Ga}_{0.91}\text{N}:\text{Mg}$ film was much reduced.

With the assumption of quasiequilibrium for the free charges, the reduced slope of the absorption edge prevents a peak from forming in the photoluminescence (PL) emission near the band-gap energy under continuous-wave (cw) excitation.¹⁸ Fitting the absorption edges to an exponential function $\exp(\gamma h\nu)$ gives $\gamma \approx 80 \text{ eV}^{-1}$ for the GaN film and

$\gamma \approx 18 \text{ eV}^{-1}$ for the $\text{Al}_{0.09}\text{Ga}_{0.91}\text{N}:\text{Mg}$ film. Through the van Roosbroeck–Shockley relation, the spontaneous emission spectrum $S(h\nu)$ and $\alpha(h\nu)$ are proportional to one another,¹⁹

$$S(h\nu) \propto (h\nu)^2 \alpha(h\nu) \exp\left(\frac{-h\nu}{kT}\right). \quad (6)$$

For a peak to appear in the spontaneous emission, $dS/d(h\nu) = 0$, requires that $\gamma \approx 1/(kT)$.²⁰ The slope of the absorption edge of the $\text{Al}_{0.09}\text{Ga}_{0.91}\text{N}:\text{Mg}$ film was too small to meet this condition, and under cw excitation no peak in the PL emission was detected in the wavelength range of 330–600 nm. In contrast, the GaN film had a slope $\gamma \approx 1/(kT)$ and correspondingly had a PL peak.⁶

In summary, the AlN buffer layer resulted in pinching of the inference fringes in the optical transmission spectrum of a $\sim 0.4\text{-}\mu\text{m}$ -thick p -type $\text{Al}_{0.09}\text{Ga}_{0.91}\text{N}$ layer heavily doped with Mg. Analysis of the transmission spectrum that included the effect of the buffer layer allowed the refractive index and absorption coefficient to be determined. The resulting index values agreed with independent measurements made by prism coupling to the layer. Through the application of detailed balance, the small slope of the band-edge absorption was found to be consistent with the lack of a cw PL peak.

This work was supported in part by DARPA Grant No. N00014-96-1-0738 and U.S. Army Research Office Grant No. DAAH04-96-0076.

- ¹L. Sugiura, M. Suzuki, and J. Nishio, Appl. Phys. Lett. **72**, 1748 (1998).
- ²M. J. Bergmann and H. C. Casey, Jr., J. Appl. Phys. **84**, 1196 (1998).
- ³D. Hofstetter, D. P. Bour, R. L. Thornton, and N. M. Johnson, Appl. Phys. Lett. **70**, 1650 (1997).
- ⁴D. Brunner, H. Angerer, E. Bustarret, F. Freudenberg, R. Höpler, R. Dimitrov, O. Ambacher, and M. Stutzmann, J. Appl. Phys. **82**, 5090 (1997).
- ⁵Measurements performed at Evans East, Inc., 666 Plainsboro Road, Suite 1236, Plainsboro, NJ 08536 (<http://www.evans-east.com/>).
- ⁶J. F. Muth, J. H. Lee, I. K. Shmagin, R. M. Kolbas, H. C. Casey, Jr., B. P. Keller, U. K. Mishra, and S. P. DenBaars, Appl. Phys. Lett. **71**, 2572 (1997).
- ⁷R. Swanepoel, J. Phys. E **16**, 1214 (1983).
- ⁸G. Yu, G. Wang, H. Ishikawa, M. Umeno, T. Soga, T. Egawa, J. Watanabe, and T. Jimbo, Appl. Phys. Lett. **70**, 3209 (1997).
- ⁹R. Swanepoel, J. Phys. E **17**, 896 (1984).
- ¹⁰M. Nowak, Thin Solid Films **254**, 200 (1995).
- ¹¹O. S. Heavens, *Optical Properties of Thin Solid Films* (Dover, New York, 1991), Chap. 4.
- ¹²N. D. Arora and J. R. Hauser, J. Appl. Phys. **53**, 8839 (1982).
- ¹³M. Born and E. Wolf, *Principles of Optics*, Sixth ed. (Pergamon, Oxford, 1989), p. 96.
- ¹⁴J. I. Cisneros, Appl. Opt. **37**, 5262 (1998).
- ¹⁵H. Y. Zhang, X. H. He, Y. H. Shih, M. Schurman, Z. C. Feng, and R. A. Stall, Appl. Phys. Lett. **69**, 2953 (1996).
- ¹⁶R. Ulrich and R. Torge, Appl. Opt. **12**, 2901 (1973).
- ¹⁷S. H. Wemple and J. A. Seaman, Appl. Opt. **12**, 2947 (1973).
- ¹⁸P. D. Southgate, J. Appl. Phys. **40**, 5333 (1969).
- ¹⁹W. van Roosbroeck and W. Shockley, Phys. Rev. **94**, 1558 (1954).
- ²⁰G. Lucovsky, A. J. Varga, and R. F. Schwarz, Solid State Comm. **3**, 9 (1965).